


Cite this: *Chem. Sci.*, 2024, 15, 2996 All publication charges for this article have been paid for by the Royal Society of Chemistry

# A DNazymes-in-droplets assay for *Burkholderia gladioli pathovar cocovenenans* with single-bacterium sensitivity†

Xiaoqian Li, Yangyang Chang, Yunping Wu and Meng Liu \*

Foodborne pathogens pose a serious risk to human health, and the simple and rapid detection of such bacteria in complex food matrices remains challenging. Herein, we present the selection and characterization of a novel RNA-cleaving fluorogenic DNzyme, named RFD-BC1, with exceptional specificity for *Burkholderia gladioli* pv. *cocovenenans* (*B. cocovenenans*), a pathogen strongly associated with fatal food poisoning cases. RFD-BC1 was activated by a protein secreted specifically by whole viable *B. cocovenenans* and displayed an optimum pH distinct from the selection pH, with a rate constant of approximately  $0.01 \text{ min}^{-1}$  at pH 5.0. Leveraging this newly discovered DNzyme, we developed a novel system, termed DNazymes-in-droplets (DID), that integrates droplet microfluidics to achieve the rapid and selective detection of live *B. cocovenenans* with single-cell sensitivity. We believe that the approach described herein holds promise for combating specific bacterial pathogens in food samples, offering significant potential for broader applications in food safety and public health.

Received 3rd November 2023

Accepted 15th January 2024

DOI: 10.1039/d3sc05874c

rsc.li/chemical-science

## Introduction

Outbreaks linked to foodborne and medically important bacterial pathogens cause millions of deaths and hospitalizations per year.<sup>1</sup> The environmental bacterium *Burkholderia gladioli* pv. *cocovenenans* (*B. cocovenenans*) was first discovered in 1933.<sup>2,3</sup> *B. cocovenenans* is pervasive in the natural environment and can cause fatal food poisoning by producing a heat-stable mitochondrial toxin called bongkrekic acid (BA), which has an acute toxicity of  $1.41 \text{ mg kg}^{-1}$  (LD50 by intravenous injection in mice).<sup>4–6</sup> BA can efficiently inhibit the mitochondrial adenine nucleotide translocator, leading to human death.<sup>4–6</sup> Outbreaks of BA food poisoning have been reported in Indonesia, Mozambique, and certain regions of China, with mortality rates reaching 40–60%.<sup>7–10</sup> The most recent lethal food poisoning case was reported in Heilongjiang Province, China, in October 2020, resulting in nine deaths, with a fatality rate of 100%.<sup>10</sup> Therefore, early and accurate detection of live pathogens is essential to prevent potential outbreaks and minimize the spread of epidemics.

Although traditional microbiological culture is the gold standard for bacterial detection, it is time-consuming and can take days to weeks.<sup>11</sup> Immunological and polymerase chain

reaction (PCR) techniques offer faster and more sensitive detection but require costly instrumentation and trained personnel.<sup>12</sup> Most importantly, they are unable to accurately distinguish live pathogens from dead ones, one of the greatest limitations in food safety and medical diagnostics. Therefore, there is a pressing need to develop rapid, accurate, inexpensive and sensitive methods for whole viable food-borne pathogen detection.

Various catalytically active DNA molecules, also known as deoxyribozymes or DNA enzymes, have been identified through *in vitro* selection from random sequence DNA pools.<sup>13–17</sup> RNA-cleaving DNazymes (RCDs) represent a widely studied class of deoxyribozymes<sup>18–22</sup> and have been successfully used as fluorescent biosensors for various live bacterial pathogens, including *Escherichia coli*, *Clostridium difficile*, *Helicobacter pylori*, *Klebsiella pneumoniae*, *Legionella pneumophila*, *Salmonella typhimurium*, *Staphylococcus aureus*, and *Fusobacterium nucleatum*.<sup>23–31</sup> A major advantage of RCD-based assays is that RCDs are activated by a specific protein target left behind by metabolically active cells, making them ideal for live pathogen detection. In light of these successes, this study aimed to explore the feasibility of utilizing RCDs as effective molecular recognition elements for live *B. cocovenenans*.

In this study, we report the *in vitro* selection and characterization of RNA-cleaving fluorogenic DNazymes (RFDs) that selectively recognize *B. cocovenenans*. Detailed features, including fluorescence signaling, kinetics, metal-ion specificities, and pH dependences, were thoroughly investigated. Notably, we found that even though the *in vitro* selection was conducted at pH 7.0, the RFDs exhibited high catalytic activity

School of Environmental Science and Technology, Key Laboratory of Industrial Ecology and Environmental Engineering (Ministry of Education), Dalian University of Technology, Dalian POCT Laboratory, Dalian, 116024, China. E-mail: mliu@dlut.edu.cn

† Electronic supplementary information (ESI) available. See DOI: <https://doi.org/10.1039/d3sc05874c>

at pH 5.0, showing a significant  $\sim 3$ -fold rate enhancement. To our knowledge, this is the first instance of bacteria-responsive RCDs that function optimally at low pH. This feature enhances the inherent chemical stability of RNA phosphodiester bonds, making RCDs more suitable for practical applications. Furthermore, we found that a *trans*-acting RFD variant also exhibited catalytic activity, with an apparent rate constant of  $0.01 \text{ min}^{-1}$ . Finally, we present a biosensing platform termed DNazymes-in-droplets (DID), which enables the selective detection of viable *B. cocovenenans* at single-cell sensitivity in culture- and amplification-free reactions within 2 h.

## Results and discussion

### *In vitro* selection of fluorogenic DNazymes activated by *B. cocovenenans*

The detailed procedure for the *in vitro* selection is provided in the ESI.† As depicted in Fig. 1a, the DNA library consisted of a 5' primer-binding site (5' PBS), a 70-nucleotide (nt) random region ( $N_{70}$ ), a 3' primer-binding site (3' PBS), and an RNA-containing DNA substrate (RDS). The RDS contained one ribonucleotide, rA, flanked by a pair of modified deoxy-ribonucleotides, one labelled with fluorescein (F) and the other

with DABCYL (Q). In the absence of *B. cocovenenans*, the DNzyme remained inactivated (Fig. 1b). In contrast, in the presence of live *B. cocovenenans*, the DNzyme cleaved the single RNA moiety in the RDS, causing fluorescence enhancement. This RNA-cleaving fluorogenic DNzyme for *B. cocovenenans* was termed RFD-BC.

Before the selection process, a crude extracellular mixture (CEM) from viable *B. cocovenenans* (named CEM-BC) was prepared by removing cells grown overnight in Luria Bertani medium (LB). Our *in vitro* selection strategy is schematically summarized in Fig. S1.† Initially, a pool of approximately  $10^{14}$  DNA sequences was incubated in the selection buffer ( $1 \times \text{SB}$ ; 50 mM HEPES, 150 mM NaCl, 15 mM  $\text{MgCl}_2$ , and 0.01% Tween 20, pH 7.0) for 5 h at room temperature. This negative selection step served to eliminate any self-cleaving DNazymes. The uncleaved DNA molecules were then purified by 10% denaturing polyacrylamide gel electrophoresis (dPAGE) and subsequently incubated with the positive selection target, CEM-BC, in  $1 \times \text{SB}$  for 2 h. The cleaved DNA products were purified by dPAGE, amplified by PCR, and used for the next selection cycle.

A total of 14 selection iterations were conducted. The round-14 DNA pool underwent deep sequencing, and the top 5 sequences were chemically synthesized (Table S1†). We then tested the RNA-cleaving activities of these sequences in the presence of CEM-BC. As shown in Fig. 1c, a DNzyme named RFD-BC1 exhibited the highest cleavage activity (20%). The sequence of RFD-BC1, provided in Fig. 1d, was selected for further investigation. We also tested the real-time fluorescence signalling capability of RFD-BC1 (Fig. 1e). RFD-BC1 demonstrated a significant fluorescence signal in the presence of CEM-BC, while no fluorescence signal enhancement was observed in  $1 \times \text{SB}$  alone.

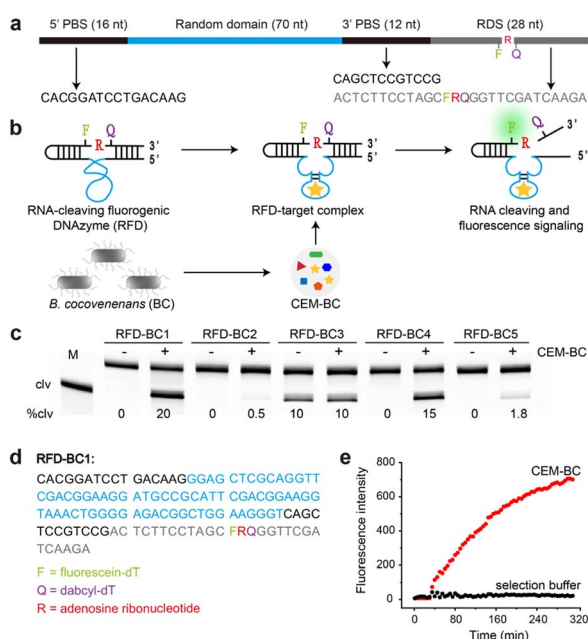


**Fig. 1** (a) The DNA library construct used in the *in vitro* selection. The construct is organized in the 5'–3' direction as 5' primer binding site (5' PBS), random domain, 3' PBS, and RNA-containing DNA substrate (RDS). F = fluorescein-dT, Q = dabcyl-dT, rA = adenosine ribonucleotide. (b) Working principle of RNA-cleaving fluorogenic DNazymes (RFDs). Upon binding to the target present in CEM-BC, the RFD cleaves the RDS at a lone RNA linkage surrounded by a closely spaced F–Q pair, thus generating a significant fluorescence signal. (c) 10% denaturing polyacrylamide gel electrophoresis (10% dPAGE) analysis of the cleavage reaction mixtures of the top 5 RFDs and CEM-BC. Reaction time: 2 h. M = DNA marker, clv = cleaved, %clv = cleavage percentage. (d) The sequence of RFD-BC1. (e) Real-time fluorescence signaling of RFD-BC1 in the presence of CEM-BC.

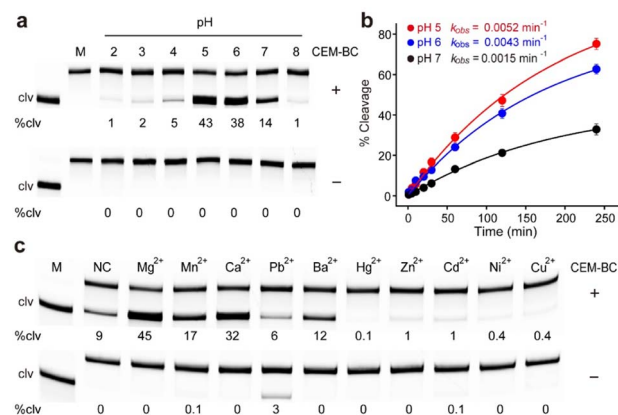


**Fig. 2** (a) pH-dependent cleavage activity of RFD-BC1. M = DNA marker, clv = cleaved, %clv = cleavage percentage. (b) Kinetic responses of RFD-BC1 at pH 5.0, 6.0 and 7.0, respectively. The solution pH was controlled with buffering reagents (each used at 50 mM): citrate for pH 2.0–3.0, acetate for pH 4.0–5.0, MES for pH 6.0, and HEPES for pH 7.0–8.0. The observed rate constant ( $k_{\text{obs}}$ ) is given in the graph. Data are represented as mean  $\pm$  s.d. ( $n = 3$ ). (c) Effect of divalent metal ions on the responses of RFD-BC1 to CEM-BC. NC: negative control, referring to the cleavage reaction performed in 50 mM acetate (pH 5.0) containing 0.01% Tween 20.



### RFD-BC1 with metal ion specificities and pH dependences

We examined the effect of pH on the catalytic efficiency of RFD-BC1 (Fig. S2†). As shown in Fig. 2a, RFD-BC1 demonstrated catalytic activity across a range of pH values (2.0 to 8.0) in the presence of CEM-BC. Notably, the highest efficiency was observed at pH 5.0, with 43% cleavage. For comparison, we determined the observed rate constants ( $k_{\text{obs}}$ ) for RFD-BC1 at pH 5.0, 6.0 and 7.0 to be  $0.52 \times 10^{-2}$ ,  $0.43 \times 10^{-2}$ , and  $0.15 \times 10^{-2} \text{ min}^{-1}$ , respectively (Fig. 2b). To our knowledge, most bacteria-responsive DNAzymes were derived to perform catalysis under neutral conditions.<sup>23–31</sup> However, several deoxy-ribozymes and ribozymes that can catalyze chemical reactions at acidic pH have also been reported.<sup>32–35</sup> The existence of this RFD-BC1 further indicates that neither the molecular recognition nor catalytic properties of nucleic acids are lost in acidic environments. At low pH, nucleic acid protonation can favor the structural folding of DNAzyme or participate in the cleavage reaction. We also tested the cleavage activity of RFD-BC1 at different temperatures (Fig. S3†). Robust cleavage activity was observed at 25 °C.

Considering the importance of metal ions in achieving high catalytic efficiency for various DNAzymes,<sup>36,37</sup> the effect of monovalent metal ions ( $\text{Na}^+$ ,  $\text{Li}^+$ ,  $\text{K}^+$ ,  $\text{Cs}^+$ , and  $\text{NH}_4^+$ ) on RFD-BC1 activity was studied (Fig. S4†). Interestingly, RFD-BC1 displayed catalytic activity in the presence of CEM-BC, even in the absence of monovalent metal ions, resulting in 11% cleavage.  $\text{Li}^+$ ,  $\text{Cs}^+$ , and  $\text{NH}_4^+$  induced strong cleavage (20–26%) in the presence of CEM-BC, while  $\text{Na}^+$  and  $\text{K}^+$  led to reduced activity (3–5%). The effects of divalent metal ions ( $\text{Mg}^{2+}$ ,  $\text{Mn}^{2+}$ ,  $\text{Ca}^{2+}$ ,  $\text{Pb}^{2+}$ ,  $\text{Ba}^{2+}$ ,  $\text{Hg}^{2+}$ ,  $\text{Zn}^{2+}$ ,  $\text{Cd}^{2+}$ ,  $\text{Ni}^{2+}$ , and  $\text{Cu}^{2+}$ ) on RFD-BC1 activity were also investigated (Fig. 2c). RFD-BC1 displayed non-metal-selective behaviour, exhibiting high catalytic activity with  $\text{Mg}^{2+}$ ,  $\text{Mn}^{2+}$ ,  $\text{Ca}^{2+}$  and  $\text{Ba}^{2+}$  (causing 12–45% of cleavage), and reduced activity with  $\text{Zn}^{2+}$ ,  $\text{Cd}^{2+}$ ,  $\text{Ni}^{2+}$ , and  $\text{Cu}^{2+}$  (causing 0.1–1% of cleavage), while remaining inactive in the presence of  $\text{Hg}^{2+}$ . Notably,  $\text{Pb}^{2+}$  induced weak cleavage (3%) in the absence of CEM-BC. Taken together, these results suggest that DNAzymes have successfully evolved to be activated by live *B. cocovenenans*, aligning with the objective of the SELEX experiment. All subsequent experiments were carried out using a reaction buffer (1× RB) composed of 50 mM acetate (pH 5.0 at 25 °C), 15 mM  $\text{MgCl}_2$ , and 0.01% Tween 20.

### RFD-BC1 is likely activated by a secreted protein in live *B. cocovenenans*

We next investigated the cleavage reactions of RFD-BC1 with CEM-BC and the crude intracellular mixture produced by *B. cocovenenans* (CIM-BC, see the SI for details). The results revealed that RFD-BC1 exhibited much stronger cleavage with CEM-BC than with CIM-BC (46% vs. 8%, Fig. S5†), suggesting that CEM-BC indeed contained a much higher amount of the target. To determine the nature of the targets in CEM-BC (*i.e.*, proteins, peptides or small-molecule metabolites), CEM-BC was treated with sodium dodecyl sulfate (SDS) and proteinase K (PK). As shown in Fig. 3a, no cleavage activity was observed, suggesting that the target is likely a protein. We then

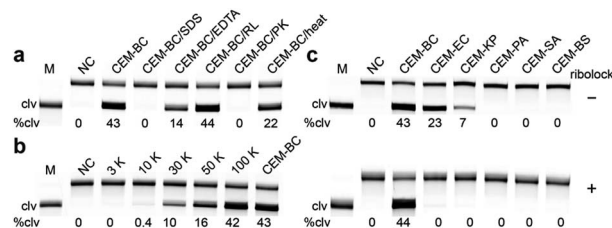


Fig. 3 (a) Responses of RFD-BC1 to CEM-BC pre-treated with SDS, EDTA, ribolock (RL, RNase inhibitor), proteinase K (PK) and heat denaturation (10 min at 90 °C). M = DAN marker, clv = cleaved, %clv = cleavage percentage. (b) Estimation of the molecular weight of the secreted protein target. CEM-BC was passed through molecular weight sizing columns, and the filtrates were then tested for reactivity with RFD-BC1. (c) Responses of RFD-BC1 to the CEMs from various bacteria, including *Escherichia coli* (EC), *Klebsiella pneumoniae* (KP), *Pedococcus acidilactici* (PA), *Staphylococcus aureus* (SA), and *Bacillus subtilis* (BS) in the absence and presence of ribolock. The reaction time for all the cleavage reactions was 2 h.

investigated whether the protein target could be a ribonuclease present in CEM-BC. However, adding an RNase inhibitor to CEM-BC did not reduce the activity of RFD-BC1 (44% cleavage). Moreover, when CEM-BC was denatured at 90 °C for 10 min, it still effectively activated RFD-BC1 (22% cleavage), suggesting the thermal stability of the protein target. In addition, RFD-BC1 exhibited reduced activity with CEM-BC containing 15 mM EDTA (14% cleavage). To estimate the molecular weight of the target protein, we conducted a molecular sizing experiment, revealing that the protein fell within the range of 10 000 to 30 000 Daltons (Fig. 3b). This conclusion was drawn because the 10 kDa filtrate of CEM-EC did not cause cleavage of RFD-BC1.

We examined the response of RFD-BC1 to CEM samples produced by six viable bacterial cells. As shown in Fig. 3c, *Escherichia coli* BL21 (EC) and *Klebsiella pneumoniae* (KP) were also capable of activating RFD-BC1, leading to nonspecific cleavage products. However, the addition of an RNase inhibitor (*i.e.*, ribolock) completely inhibited the nonspecific cleavage activity of RFD-BC1. Therefore, we hypothesized that the observed nonspecific cleavage was most likely due to the presence of various RNases expressed by bacteria. The addition of the RNase inhibitor will significantly suppress the activity of RNases, thus improving the specificity.<sup>28</sup> Previously, it was demonstrated that removal of the internal F and Q modifications can efficiently improve the activity but reduce the specificity of the DNAzyme.<sup>28</sup> However, we found that the presence of the F and Q modifications had no effect on the catalytic activity (with a  $k_{\text{obs}}$  of  $0.006 \text{ min}^{-1}$ ) and specificity of RFD-BC1 (Fig. S6†). These experiments indicate that this DNAzyme is highly specific to the protein target secreted in *B. cocovenenans*.

The fluorescence response of RFD-BC1 in the presence of different concentrations of live *B. cocovenenans* was also examined (Fig. S7†). Remarkably, RFD-BC1 was able to detect *B. cocovenenans* at concentrations as low as  $10^3$  colony-forming units (CFU) per mL without requiring cell culture. This detection limit is comparable to those reported for other bacteria-responsive DNAzymes, such as those for *Escherichia coli* ( $10^4$





CFU mL<sup>-1</sup>),<sup>23,24</sup> *Helicobacter pylori* (10<sup>4</sup> CFU mL<sup>-1</sup>),<sup>27</sup> and *Staphylococcus aureus* (10<sup>3</sup> CFU mL<sup>-1</sup>).<sup>26</sup>

### Sequence optimization by nucleotide truncation

We then investigated the possibility of shortening the sequence of RFD-BC1. We found that at least 45 nucleotides could be deleted from the 5' end without compromising its functionality. The resulting shortened version, named RFD-BC1S1 (Fig. 4a), consists of a single-stranded region (S1), two short duplexes (P1 and P2), two hairpin loops (L1 and L2), and one interhelical unpaired element (J1/2). Note that it is possible that S1 is directly involved in some tertiary interactions that are essential for structure folding and catalytic function. The existence of P2 was further confirmed by using an engineered *trans*-acting DNzyme system, denoted RFD-BC1T1, which efficiently cleaved the matching external RDS (Fig. 4b). Fig. 4c shows the cleavage of RDS by RFD-BC1S1 and RFD-BC1T1 in the presence of CEM-BC, with the  $k_{\text{obs}}$  of 0.008 min<sup>-1</sup> and 0.01 min<sup>-1</sup>, and the final cleavage yield of 82% and 80% at 25 °C, respectively (Fig. S8†). We also tested whether RFD-BC1T1 could perform multiple-turnover cleavage reactions (Fig. S9†). It was indicated that approximately 12 turnovers were obtained after a 12 h incubation wherein a 100-fold excess of substrate was present (Fig. 4d). These data indicate that RFD-BC1T1 is a very efficient DNzyme.

To assess the essentiality of each nucleotide within RFD-BC1T1, 30 mutant constructs of RFD-BC1T1 were examined (Fig. 5 and S10†). (1) For S1, the remaining nucleotides from T4 to T9 are important as mutation to each of them significantly reduced %clv (M2 and M3). In contrast, G1, C2, and A3 can be

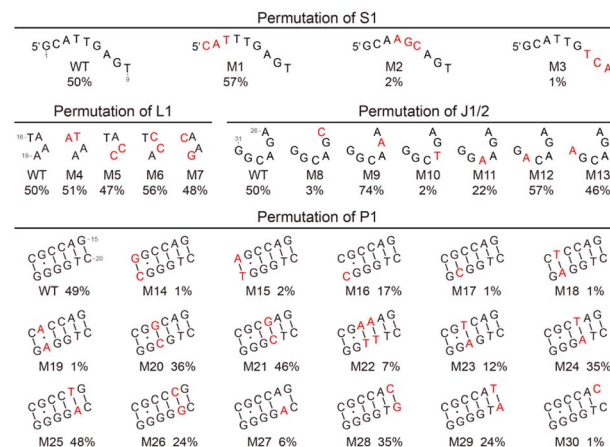


Fig. 5 RFD-BC1T1 with permuted S1, L1, J1/2, and P1 elements. Nucleotides shown in red are the actual altered nucleotides in each construct in comparison to RFD-BC1T1. WT: wild-type sequence. %clv is shown for each construct.

mutated (M1). (2) For L1, T16, A17, A18, and A19 can tolerate mutations (M4, M5, M6, and M7). (3) For J1/2, A26, A28, and C29 are important nucleotides because mutating any of these nucleotides caused a noticeable reduction in %clv (M8, M10, and M11). However, G27, G30, and G31 can be mutated (M9, M12, and M13); interestingly, mutation of G27 to A27 could significantly enhance the %clv from 50% to 74%. (4) For P1, mutating the C10–G25 pair into the G–C pair (M14), A–T pair (M15), or C–C mismatch (M16) significantly reduced the %clv. The G11–G24 mismatch is very important, and replacing it with either the G–C pair (M17), T–A pair (M18) or A–A mismatch (M19) caused noticeable %clv reduction. The C12–G23 pair is also important as substituting it with a G–C pair (M20), a T–A pair (M22), or a A–T pair (M23) always reduced %clv. The C13–G22 pair could be changed to a G–C pair (M21) but not a T–A pair (M24). When the A14–T21 pair was mutated into a T–A pair (M25), no reduction in %clv was observed; however, if it was altered to the C–G pair (M26) or A–A mismatch (M27), then %clv dropped. For the G15–C20 pair, the substitution with a C–G pair (M28) or a T–A pair (M29) or a C–C mismatch (M30) can also result in the reduction of %clv.

### The DNzymes-in-droplets assay for bacteria detection

We then designed a rapid and highly sensitive sensing system. Droplet microfluidic devices are well known for enabling the encapsulation of single molecules within microdroplets, making them ideal for achieving ultrasensitive biological detection in a short period.<sup>38,39</sup> Here, we introduce the DNzymes-in-Droplets (DID) assay, which integrates DNzyme-based sensors, droplet encapsulation and digital counting.

The fundamental operation and working principle of the DID assay are illustrated in Fig. 6. Specifically, the cell lysates from a particular viable bacterial cell are mixed with fluorogenic DNzymes in the microfluidic chip and immediately encapsulated into up to ~30 000 droplets. Within these droplets, the following sequence of reactions takes place: (1) recognition

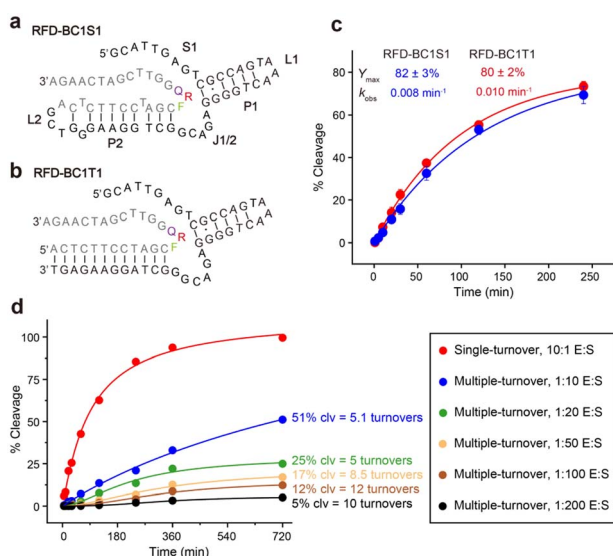
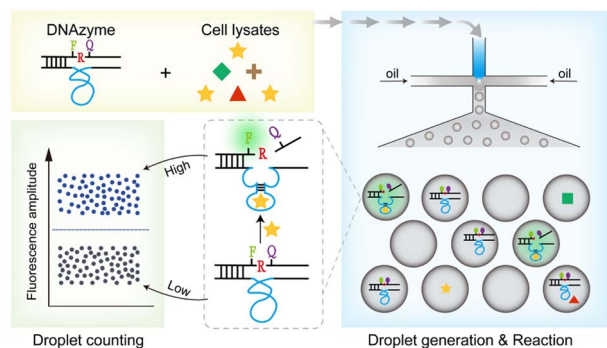


Fig. 4 (a) Proposed secondary structure of RFD-BC1S1. Individual elements are marked as P (pairing region), L (loop), and J (junction between two pairing regions). RDS sequences are highlighted in grey. (b) A *trans*-acting DNA enzyme, RFD-BC1T1. (c) Kinetic analysis of RFD-BC1S1 and RFD-BC1T1. Data are represented as mean  $\pm$  s.d. ( $n = 3$ ). (d) Analysis of RFD-BC1T1 for multiple turnover. The number of turnovers was calculated from the final %cleavage at 720 min.





**Fig. 6** Working principle of DNAzymes-in-droplets (DID) assay for live bacteria detection. Cell lysates and RNA-cleaving fluorogenic DNAzymes are mixed and then encapsulated into the water-in-oil microdroplets, where DNAzymes produce high fluorescent signals in the droplets that contain the protein target. Droplets are then analysed using the counting system that can accurately distinguish single-fluorescent droplets from these non-fluorescent droplets.

occurs between the DNAzymes and the protein targets; (2) cleavage of an RNA-containing substrate ensues upon target binding; and (3) fluorescence dequenching occurs as a result of cleavage. Subsequently, the droplets are imaged and analysed using the on-chip counting system.

We first examined the DID assay using *trans*-acting RFD-BC1T1. The droplet microfluidic system generated uniform, picolitre-sized liquid droplets (typically 90  $\mu\text{m}$  in diameter)

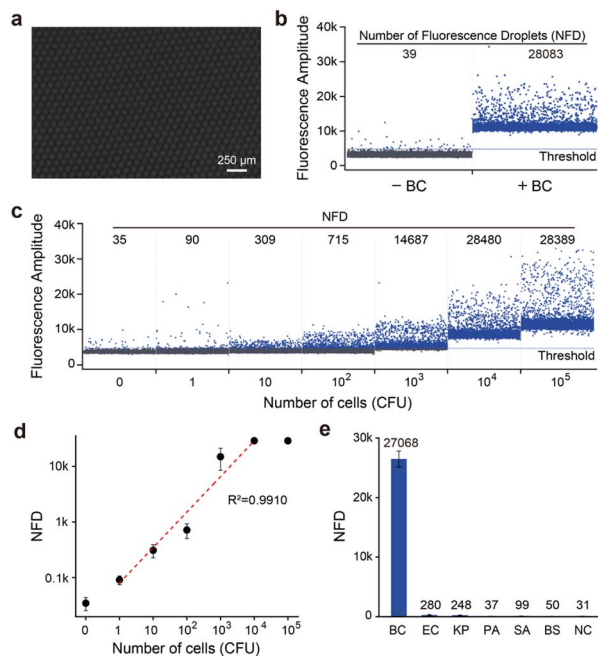


**Fig. 7** (a) Representative microscopy images showing uniform picoliter-sized droplets. Scale bar: 250  $\mu\text{m}$ . (b) Feasibility of bacterial detection using the DID assay. (c) Fluorescence response of the DID assay to various concentrations of BC cells. (d) NFD as a function of the number of bacteria (CFU). The error bars represent standard deviations of three independent experiments. (e) Specificity of the DID assay. The concentration of each bacterium was  $10^5$  CFU.

(Fig. 7a). Positive droplets, containing BC cell lysates and RDS/RFD-BC1T1, displayed a high fluorescence signal (Fig. 7b), while control droplets containing only RDS/RFD-BC1T1 did not exhibit any obvious signal above the automated threshold (estimated by the Crystal Miner software that maximizes the inter-class variance and minimizes the intra-class variance). We then determined the minimal DNAzyme reaction time required in droplets. We observed the time course of the number of fluorescent droplets (NFD), which reached a plateau at approximately 60 min (Fig. S11<sup>†</sup>). The DID assay demonstrated the capability of quantifying target BC over a broad concentration range of 1 to 10 000 CFU  $\text{mL}^{-1}$  within 2 h (Fig. 7c). This time frame included the cell lysing time (<10 min), droplet generation time ( $\sim 45$  min), DNAzyme reaction time (60 min), and droplet counting and analysis time (<5 min). Therefore, our strategy significantly reduced the assay time compared with the reported “Integrated Comprehensive Droplet Digital Detection” (IC 3D) method (with a total assay time of  $\sim 4$  h).<sup>38</sup> Because a whole bacterial cell produces many thousands of potential protein targets, a large number of fluorescent droplets can be observed even at low concentrations. The DID assay exhibited single-cell sensitivity (Fig. 7d) and excellent selectivity for its cognate target (Fig. S12<sup>†</sup>). None of the CEM samples from other randomly selected live bacteria, such as EC, KP, PA, SA, and BS, produced a detectable NFD (Fig. 7e).

To challenge the developed assay, *B. cocovenenans* was analysed in a matrix of the *Tremella fuciformis* mushroom, a traditional Chinese food associated with *B. cocovenenans* food poisoning outbreaks. Samples spiked with 50, 500, and 5000 living BC cells were tested in this experiment (Fig. S13<sup>†</sup>). The results exhibited a good correlation between the detected number of bacterial cells and the actual concentration of target bacteria spiked into the sample, with calculated recovery values ranging from 76% to 107%. These results demonstrated the capability of our assay to accurately detect target bacteria in food samples.

## Conclusions

In this study, we present the first successful derivation of RNA-cleaving DNAzymes that are activated by *B. cocovenenans*. We identified a set of DNAzymes with specific recognition for *B. cocovenenans*, among which one notable DNAzyme is RFD-BC1. Under the reaction conditions of 50 mM citrate (pH 5.0 at 25  $^{\circ}\text{C}$ ), 15 mM  $\text{MgCl}_2$ , and 0.01% Tween 20, RFD-BC1 exhibited a  $k_{\text{obs}}$  of  $0.0052 \text{ min}^{-1}$ . Moreover, RFD-BC1 can be used as a sensitive DNAzyme sensor capable of producing a detectable signal at concentrations as low as  $10^3$  CFU  $\text{mL}^{-1}$ . In addition, we found that truncating RFD-BC1 produced a *trans*-acting DNAzyme system, termed RFD-BC1T1, which displays a  $k_{\text{obs}}$  of  $0.01 \text{ min}^{-1}$ . Finally, we developed an on-chip droplet counting system that integrates DNAzyme-based molecular recognition and droplet microfluidics, enabling the rapid and selective detection of live *B. cocovenenans* with single-cell sensitivity. The high-resolution structural studies of RFD-BC1 will be the subject of a future investigation, which will enable us to understand the detailed mechanisms of catalysis.<sup>40,41</sup> We



believe that the strategies demonstrated here have the potential to expand the practical utility of DNAzymes in combating various food-borne and medically important pathogens. These findings mark a significant advancement in developing sensitive and efficient detection methods for bacterial pathogens, thus contributing to efforts to prevent outbreaks and minimize the spread of epidemics caused by such pathogens.

## Data availability

Experimental data is available in the ESI online.†

## Author contributions

M. L. applied for the funding. M. L. conceived the idea and supervised the project. X. Q. L. performed the experiments and data collection. X. Q. L., Y. Y. C., Y. P. W., and M. L. analyzed the data. X. Q. L., Y. Y. C., Y. P. W., and M. L. wrote the manuscript.

## Conflicts of interest

There are no conflicts to declare.

## Acknowledgements

This work was supported by the the National Key R&D Program of China (No. 2023YFC3205804) and Dalian Science and Technology Innovation Fund (2023YGZD06).

## Notes and references

- 1 World Health Organization, *WHO Estimates of the Global Burden of Foodborne Diseases: Foodborne Disease Burden Epidemiology Reference Group 2007-2015*, WHO, 2015, p. 255.
- 2 P. A. Vandamme, A. G. Johannes, H. C. Cox and W. Berends, *Recl. Trav. Chim. Pays-Bas*, 1960, **79**, 255–267.
- 3 B. Dose, C. Ross, S. P. Niehs, K. Scherlach, J. P. Bauer and C. Hertweck, *Angew. Chem., Int. Ed.*, 2020, **59**, 21535–21540.
- 4 M. Anwar, A. Kasper, A. R. Steck and J. G. Schier, *J. Med. Toxicol.*, 2017, **13**, 173–179.
- 5 N. Moebius, C. Ross, K. Scherlach, B. Rohm, M. Roth and C. Hertweck, *Chem. Biol.*, 2012, **19**, 1164–1174.
- 6 S. Fujita, M. Suyama, K. Matsumoto, A. Yamamoto, T. Yamamoto, Y. Hiroshima, T. Iwata, A. Kano, Y. Shinohara and M. Shindo, *Tetrahedron*, 2018, **74**, 962–969.
- 7 E. S. Gudo, K. Cook, A. M. Kasper, A. Vergara, C. Salomao, F. Oliveira, H. Ismael, C. Saeze, C. Mosse, Q. Fernandes, S. O. Viegas, C. S. Baltazar, T. J. Doyle, E. Yard, A. Steck, M. Serret, T. M. Falconer, S. E. Kern, J. L. Brzezinski, J. A. Turner, B. L. Boyd, I. V. Jani and Chitima Investigation Group, *Clin. Infect. Dis.*, 2018, **66**, 1400–1406.
- 8 J. Li, L. Zhou, C. Long, L. Fang, Q. Chen, Q. Chen, J. Liang, Y. Yang, H. Zhu, Z. Chen, S. Gao, Z. Li, Q. Li, Q. Huang and Y. Zhang, *J. Food Prot.*, 2019, **82**, 1650–1654.
- 9 Z. Peng, T. Dottorini, Y. Hu, M. Li, S. Yan, S. Fanning, M. Baker, J. Xu and F. Li, *Front. Microbiol.*, 2021, **12**, 628538.
- 10 Y. Yuan, R. Gao, Q. Liang, L. Song, J. Huang, N. Lang and J. Zhou, *China CDC Weekly (CCDC Weekly)*, 2020, **2**, 975–978.
- 11 M. Zourob, S. Elwary and A. Turner, *Principles of Bacterial Detection: Biosensors, Recognition Receptors and Microsystems*. Springer, NY, USA, 2008.
- 12 V. Velusamy, K. Arshak, O. Korostynska, K. Oliwa and C. Adley, *Biotechnol. Adv.*, 2010, **28**, 232–254.
- 13 R. R. Breaker and G. F. Joyce, *Chem. Biol.*, 1994, **1**, 223–229.
- 14 M. V. Sednev, V. Mykhailiuk, P. Choudhury, J. Halang, K. E. Sloan, M. T. Bohnsack and C. Höbartner, *Angew. Chem., Int. Ed.*, 2018, **57**, 15117–15121.
- 15 V. Dokukina and S. K. Silverman, *Chem. Sci.*, 2012, **3**, 1707–1714.
- 16 Y. Wang, Y. Wang, D. Song, X. Sun, Z. Li, J.-Y. Chen and H. Yu, *Nat. Chem.*, 2022, **14**, 350–359.
- 17 R. Pandey, D. Chang, M. Smieja, T. Hoare, Y. Li and L. Soleymani, *Nat. Chem.*, 2021, **13**, 895–901.
- 18 S. K. Silverman, *Acc. Chem. Res.*, 2009, **42**, 1521–1531.
- 19 E. M. McConnell, I. Cozma, Q. Mou, J. D. Brennan, Y. Lu and Y. Li, *Chem. Soc. Rev.*, 2021, **50**, 8954–8994.
- 20 H. Wang, H. Wang, Q. Wu, M. Liang, X. Liu and F. Wang, *Chem. Sci.*, 2019, **10**, 9597–9604.
- 21 Y. Xiang, Z. Wang, H. Xing and Y. Lu, *Chem. Sci.*, 2013, **4**, 398–404.
- 22 K. Chiba, T. Yamaguchi and S. Obika, *Chem. Sci.*, 2023, **14**, 7620–7629.
- 23 D. Chang, S. Zakaria, S. E. Samani, Y. Chang, C. D. M. Filipe, L. Soleymani, J. D. Brennan, M. Liu and Y. Li, *Acc. Chem. Res.*, 2021, **54**, 3540–3549.
- 24 M. M. Ali, S. D. Aguirre, H. Lazim and Y. Li, *Angew. Chem., Int. Ed.*, 2011, **50**, 3751–3754.
- 25 Z. Shen, Z. Wu, D. Chang, W. Zhang, T. Kha, C. Lee, P. Kim, B. J. Salena and Y. Li, *Angew. Chem., Int. Ed.*, 2016, **55**, 2431–2434.
- 26 M. M. Ali, R. Silva, D. White, S. Mohammadi, Y. Li, A. Capretta and J. D. Brennan, *Angew. Chem., Int. Ed.*, 2022, **61**, e202112346.
- 27 M. M. Ali, M. Wolfe, K. Tram, J. Gu, C. D. M. Filipe, Y. Li and J. D. Brennan, *Angew. Chem., Int. Ed.*, 2019, **58**, 9907–9911.
- 28 M. Rothenbroker, E. M. McConnell, J. Gu, M. L. Urbanus, S. E. Samani, A. W. Ensminger, C. D. M. Filipe and Y. Li, *Angew. Chem., Int. Ed.*, 2021, **60**, 4782–4788.
- 29 M. M. Ali, A. Slepkin, E. Peterson and W. Zhao, *ChemBioChem*, 2019, **20**, 906–910.
- 30 J. Li, S. Khan, J. Gu, C. D. M. Filipe, T. F. Didar and Y. Li, *Angew. Chem., Int. Ed.*, 2023, **62**, e202300828.
- 31 Q. Feng, S. Zakaria, D. Morrison, K. Tram, J. Gu, B. Salena and Y. Li, *Angew. Chem., Int. Ed.*, 2023, **62**, e202306272.
- 32 Z. J. Liu, S. H. J. Mei, J. D. Brennan and Y. Li, *J. Am. Chem. Soc.*, 2003, **125**, 7539–7545.
- 33 S. A. Kandadai and Y. Li, *Nucleic Acids Res.*, 2005, **33**, 7164–7175.
- 34 S. A. Kandadai, W. W. Mok, M. M. Ali and Y. Li, *Biochemistry*, 2009, **48**, 7383–7391.
- 35 V. K. Jayasena and L. Gold, *Proc. Natl. Acad. Sci. U. S. A.*, 1997, **94**, 10612–10617.



- 36 A. Ponce-Salvatierra, K. Wawrzyniak-Turek, U. Steuerwald, C. Hoebartner and V. Pena, *Nature*, 2016, **529**, 231–234.
- 37 J. Borggraefe, J. Victor, H. Rosenbach, A. Viegas, C. G. W. Gertzen, C. Wuebben, H. Kovacs, M. Gopalswamy, D. Riesner, G. Steger, O. Schiemann, H. Gohlke, I. Span and M. Etzkorn, *Nature*, 2022, **601**, 144–149.
- 38 D. K. Kang, M. M. Ali, K. X. Zhang, S. S. Huang, E. Peterson, M. A. Digman, E. Gratton and W. A. Zhao, *Nat. Commun.*, 2014, **5**, 5427.
- 39 L. Shang, Y. Cheng and Y. Zhao, *Chem. Rev.*, 2017, **117**, 7964–8040; Y. Ding, P. D. Howes and A. J. deMello, *Anal. Chem.*, 2020, **92**, 132–149.
- 40 A. Ponce-Salvatierra, K. Wawrzyniak-Turek, U. Steuerwald, C. Hoebartner and V. Pena, *Nature*, 2016, **529**, 231–234.
- 41 J. Borggraefe, J. Victor, H. Rosenbach, A. Viegas, C. G. W. Gertzen, C. Wuebben, H. Kovacs, M. Gopalswamy, D. Riesner, G. Steger, O. Schiemann, H. Gohlke, I. Span and M. Etzkorn, *Nature*, 2022, **601**, 144–149.

